1-1-2009

Response of rigid polyurethane foam-filled steel hollow columns under low velocity impact

Alexander Remennikov
University of Wollongong, alexrem@uow.edu.au

Brian Uy
brianuy@uow.edu.au

Kong Sih Ying
ksy965@uow.edu.au

8th International Conference on **SHOCK & IMPACT LOADS ON STRUCTURES**
December 2-4, 2009, Adelaide, Australia

RESPONSE OF RIGID POLYURETHANE FOAM-FILLED STEEL HOLLOW COLUMNS UNDER LOW VELOCITY IMPACT

A M Remennikov*, University of Wollongong, Australia
S Y Kong, University of Wollongong, Australia
B Uy, University of Western Sydney, Australia

Abstract

This paper presents the results of experimental investigations on rigid polyurethane foam-filled steel hollow columns under dynamic loading conditions. The 100x5 SHS mild steel and stainless steel columns with 2.85m span were simply supported at both ends. The columns were subjected to impact loads from a 600 kg falling mass in mid-span. During the tests, a high-speed data acquisition system was used to record the load history, accelerations and deflections at the mid-span and quarter-span. The dynamic results showed that the energy absorption capacity of the foam-filled steel columns increased compared to the unfilled hollow sections, but was not as high as the energy absorbed by the equivalent concrete filled columns. From the recorded acceleration data, the inertial effects of the columns under dynamic load have been investigated. The failure mode for impact loading conditions was observed. The experimental results have been used to verify finite element models of hollow and foam-filled steel columns.

Keywords: Polyurethane foam, mild steel, stainless steel, column, impact, numerical modelling

1. Introduction

Polyurethane foams generally consists of polyisocyanates reacted with polyols in the presence of a catalyst. Flexible polyurethane foams generally are used in furniture, carpet underlay, bedding and semi-flexible foams in automobiles. Rigid polyurethane foams are used for insulation in buildings. Their high energy absorption capacity has attracted increasing attention from engineers and researchers in recent years.

Shim *et al* [1] performed an investigation into the two dimensional response of polyurethane foam impact limiters. The results obtained from their investigation showed that the resistance to deformation of the foam is related to the width of the impactor and not the geometry of the impactor's nose. Tu *et al* [2] investigated the plastic deformation of rigid polyurethane foam in both vertical and transverse axes. It was found that the foam under compression has an initial region of linear elastic response up to yielding followed by a flat plateau compaction zone. With this plateau region, the foam is capable of absorbing a significant amount of energy.

Chen *et al* [3] performed compressive tests on rigid polyurethane foam with various densities under high strain rate. The results indicated that higher density foam was capable of reaching much higher stress but with a reduced strain capacity. This study also showed that under high strain rate loading, the foam attained much higher stress and strain.

Lilley and Mani [4] carried out small scale four point bending tests to investigate the application of rigid polyurethane foam on vehicle pillars under a roof-crush loading. Tests were performed on an unfilled tube and tubes filled with different foam densities. A full-scale roof-crush test was performed by modelling a pick-up truck cab using finite element software. This research concluded that rigid polyurethane foam in-fill can improve the bending strength of thin walled, hollow structures such as the B-pillars. The higher the density of polyurethane foam, the higher the strength and stiffness provided to such structures.

Ismail [5] studied the strength of a rigid polyurethane foam-filled column subjected to quasi-static oblique compression loading. The effects of different foam densities, column wall thickness and angle of oblique loading were also investigated. Experimental results showed both foam density and wall thickness are the key factors determining the crashworthiness behaviours but when the structures are exposed to oblique loading, the energy absorption capacity decreased accordingly as loading angles increased.

2. Experimental program

2.1 Material testing

Three compressive tests were carried out on 30x30x30mm rigid polyurethane foam (PUR) cubes by using an Instron universal testing machine to determine the material characteristics under monotonically increasing compressive loading. Specimens were obtained from the PUR in-fill in the columns for the dynamic three point bending tests and the density measured was approximately 200 kg/m^3.

To obtain the material properties for mild steel and stainless steel, tests utilising standard coupons were conducted by using the Instron machine at the University of Western Sydney. Three specimens were tested for each type of steel. The applied load and elongation of the specimens were recorded during the tests.

2.2 Dynamic three points bending tests

The 100x100x5mm SHS columns were subjected to dynamic three point bending tests to investigate their response characteristics. The mild steel and stainless steel columns were tested with both hollow sections and PUR filled sections. The experiment program is outlined in Table 1.

Table 1: Experiment outline for dynamic three point bending tests

Experimental program	Type of steel section	Abbreviation	Specimen
Dynamic test	Mild steel hollow section	MDH	MDH1, MDH2
	Mild steel foam filled section	MDF	MDF1, MDF2
	Stainless steel hollow section	SDH	SDH1, SDH2
	Stainless steel foam filled section	SDF	SDF1, SDF2

The dynamic three point bending test was performed using the drop hammer rig illustrated in Figure 1. The experimental setup for the dynamic test was for columns with an effective length of 2.5m simply supported at both ends. A rebound mechanism was used to control the excessive rebound of the columns under impact loading. A falling mass of 590kg was released from a 650mm height to directly impact onto the steel columns at the mid-span.

Accelerometers were mounted at the mid-span and quarter-span of the columns to record their acceleration. The mid-span displacement was measured by a wire potentiometer while the quarter-span displacement was measured by a high-speed displacement laser. A post-yield strain gauge was attached to the bottom of the column at mid-span to measure the tensile strain. The contact force between the column and the drop hammer was captured by a dynamic load cell mounted on the drop hammer. The high-speed data acquisition system was used to record the experiment data at a frequency of 100 kHz.

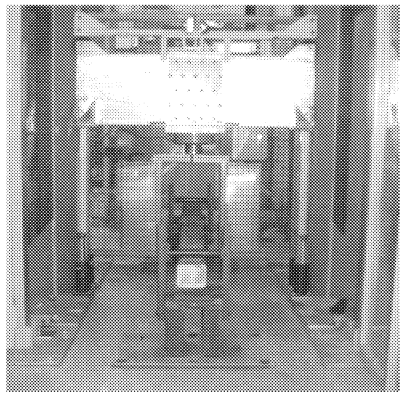

Figure 1: Dynamic three point bending test set up (drop hammer machine).

3. Experimental results

The compressive stress-strain curve of the PUR illustrated in Figure 2(a) can be classified into three zones. An initial region of elastic response until the material starts yielding at a stress of 2.2MPa, followed by a compaction zone where the strain increases while the stress remains constant. After exceeding 20% of strain, the PUR enters a densification zone where the stress increases exponentially with the strain increment.

As illustrated in Figure 2(b), the tensile stress-strain relationship for mild steel and stainless steel specimens did not demonstrate a well-defined yield stress thus the 0.2% proof stress was used to determine the yield stresses. The mild steel specimens showed a consistent stress-strain relationship and the mean yield stress was 437MPa. The stainless steel specimens displayed greater variation in their stress-strain relationships with the mean yield stress determined as 615MPa.

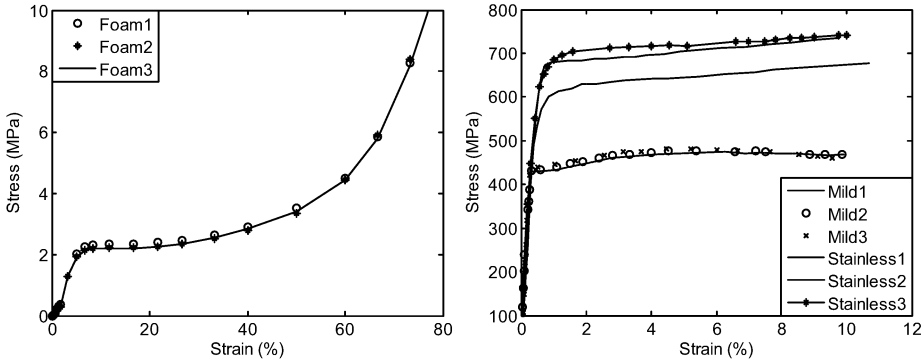

Figure 2: (a) Stress-strain curve for PUR cubes, (b) stress-strain curve for mild steel and stainless steel coupons.

The processed acceleration data for the MDH1 specimen at mid-span is illustrated in Figure 3 while the dynamic three point bending results for mild steel and stainless steel columns are presented in Figures 4 and 5 for hollow sections and foam-filled sections. The results of the concrete-filled mild steel (denoted as MDCF in Figure 4) and the stainless steel column (denoted as SDCF in Figure 5) are also included to compare the effect of different infill materials on the dynamic behaviours of these columns.

Under impact load, the resistance of the columns can be divided into an inertial component and a flexural resistance component. The inertial component of the columns is the high frequency oscillation of the contact force at the initial stage of the impact, as illustrated in Figures 7 to 10. The processed acceleration data for the MDH1 specimen at mid-span obtained by filtering out high frequency waves is shown in Figure 3. It was observed that all the specimens have similar acceleration profiles with varied magnitudes. The inertial component for all the specimens is extracted in this paper and only the flexural resistance components of the mild steel and stainless steel specimens are presented in Figures 4 and 5.

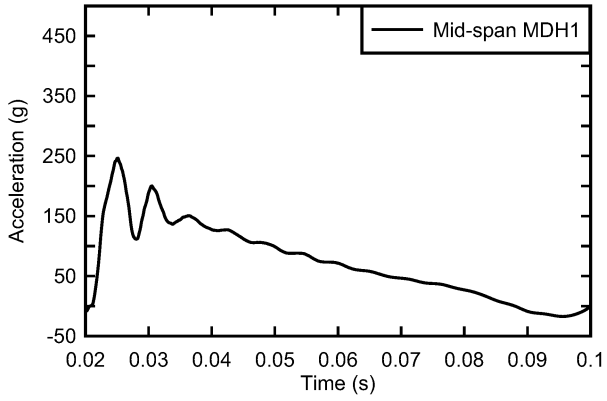

Figure 3: Acceleration recorded on mild steel hollow section MDH1 at mid-span.

From the Figure 4, it was observed that the experimental result for MDF2 showed premature failure compared to all other specimens, thus it was ignored in the analysis. It was observed that the foam-filled section MDF1 has higher strength than the hollow sections, while the concrete filled section MDCF showed the highest strength. The resistance of hollow sections reduced gradually with the increment in mid-span displacement, while for foam-filled and concrete filled columns the strength remained the same when the mid-span displacement increases.

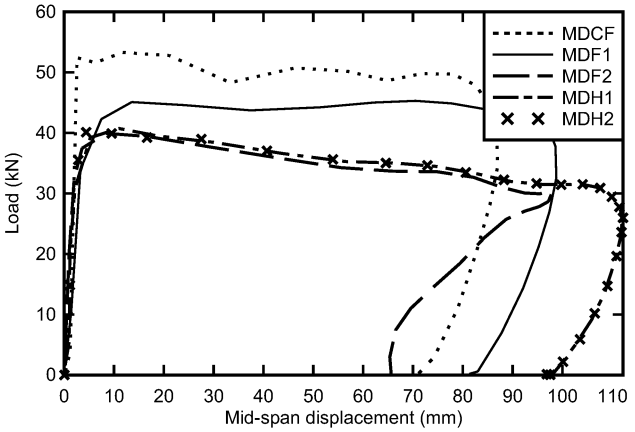

Figure 4: Flexural resistance component for mild steel columns under drop hammer impact.

Since the drop height of the hammer is the same for all the specimens, the amount of energy delivered by the hammer to the columns is the same. The amount of energy dissipated by columns is a function of the load and displacement of the specimens. Thus hollow sections showed largest deformation, the foam filled section had intermediate deformation while the concrete filled section showed the least deformation to dissipate the same amount of imparted energy. This implies that the infill-material is able to reduce the deflection of columns under impact load. The maximum flexural strength and deflection of the mild steel specimens are summarized in Table 2.

Table 2: The strength, deflection and energy absorption for mild steel sections under impact load

Mild steel specimen	Maximum load (kN)	Maximum deflection (mm)	Residual deflection (mm)	Energy absorbed at 60mm mid-span displacement (J)
MDH1	40	110	97	2233
MDH2	40	110	97	2237
MDF1	45	98	82	2547
MDF2	-	-	-	-
MDCF	53	86	71	3008

Both the hollow mild steel columns and foam filled columns failed in local buckling mode, as shown in Figure 11(b). The concrete filled mild steel column however showed no sign of local buckling due to the confinement effects of the concrete infill. The energy absorption capacity of infill materials is evaluated by comparing the total amount of energy absorbed by the mild steel columns under a 60mm mid-span displacement. The amount of energies absorbed by the columns is the areas under the resistance curve up to the 60mm mid-span displacement in Figure 3 and it is these energies that are presented in Table 2. This evaluation showed that the energy absorption capacity of the foam-filled mild steel columns increased compared to the unfilled hollow sections, but this was not as high as the energy absorbed by the equivalent concrete filled columns.

The experimental result for stainless steel foam filled column SDF1 was excluded in the analysis due to failure of the wire potentiometer as illustrated in Figure 5. Generally, stainless steel columns showed similar result patterns to the mild steel specimens, with the concrete filled column SDCF showing highest strength and least deformation. The foam filled stainless steel column SDF1 showed intermediate strength and displacement. The flexural resistance of all the stainless steel specimens remained the same or slightly increased with the increment in mid-span displacement. The maximum flexural strength and mid-span displacement of the stainless steel specimens are summarized in Table 3.

The energy absorption capacity of infill materials is evaluated by comparing the total amount of energy absorbed by the stainless steel columns under 60mm mid-span displacement. The results presented in Table 3 show that the polyurethane foam slightly increases the energy absorption of the stainless steel columns, and the concrete filled stainless steel column had the highest energy absorption capacity. Both hollow and foam filled stainless steel columns failed in local buckling of the impact zone while the concrete filled stainless steel column had no visible local buckling.

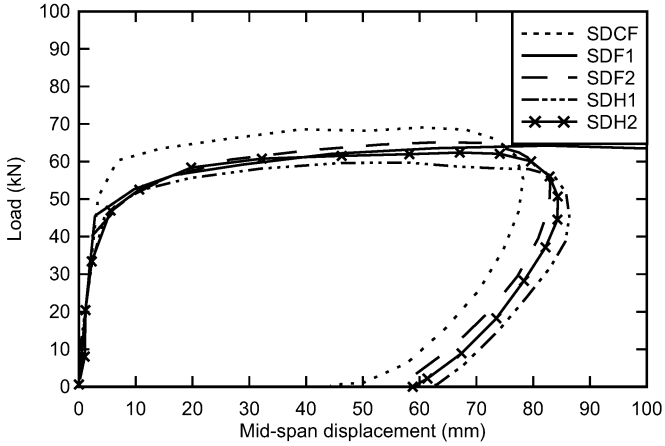

Figure 5: Flexural resistance component for stainless steel columns under drop hammer impact.

Table 3: The strength, deflection and energy absorption of mild steel and stainless steel specimens under impact load

Stainless steel specimen	Maximum load (kN)	Maximum deflection (mm)	Residual deflection (mm)	Energy absorbed at 60mm mid-span displacement (J)
SDH1	60	86	62	3288
SDH2	63	85	59	3386
SDF1	-	-	-	-
SDF2	65	83	58	3483
SDCF	70	78	44	3844

4. Numerical simulation

A quarter of the complete dynamic three points bending test setup was modelled using the explicit non-linear finite element code LS-Dyna due to its symmetry. The model consists of the drop hammer, column, roller support and the rebound mechanism as illustrated in Figure 6. The hammer, roller support and the rebound mechanism were modelled by using solid elements while the column was modelled by shell elements. The mesh size of approximately 10mm was applied for the columns in order to capture their dynamic behaviour reasonably well under impact.

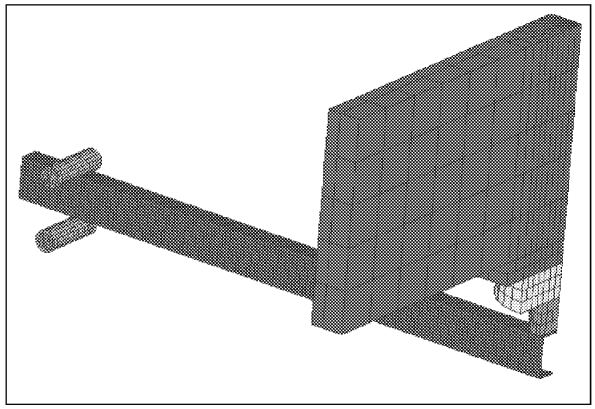

Figure 6: LS-Dyna model of the dynamic three points bending test.

For the material modelling, Material Type 24, Isotropic piecewise linear plastic model was applied for the mild steel and stainless steel columns. Values of 0.3 and 200GPa were given for Poisson's ratio and Young's modulus respectively. The stress-strain behaviours after yielding for both steels were modelled and it was found that the numerical results corresponded better with the experimental results by ignoring the Cowper-Symonds coefficients.

PUR was modelled using Material Type 83, MAT_FU_CHANG with the input Young's modulus and density 40MPa and 200kg/m^3 respectively. A nominal stress-strain curve was defined according to Figure 2(a). Recommendations by Sambamoorthy [6] such as applying a value of 0 for the tensile cut-off stress, no bulk viscosity in BVFLAG option and to use default values for other parameters were adopted in these simulations. Tensile properties of PUR were modelled according to Mullerschon's recommendations [7].

Figure 7 to Figure 10 illustrated the comparison between the predicted numerical results with the experimental results in terms of mid-span displacement and contact force. *Num.* in the figures denotes numerical while *displ.* denotes mid-span displacement. All of the predicted maximum mid-span displacements are lower than the experimental results while all of the predicted loading histories corresponding well with the experimental results.

Figure 7 and Figure 8 showed that numerical results corresponded very well with the experimental results for mild steel hollow and foam filled sections. The difference between predicted and experimental results in the maximum mid-span displacement for the hollow and foam filled section is 8% and 6% respectively. For the stainless steel hollow and foam filled sections, the predicted results corresponded reasonably well with experimental results, where the difference in maximum mid-span displacement is 17% and 15% respectively as shown in Figure 9 and 10.

From Figures 7 to 10, all the hollow and filled columns recorded high-frequency oscillations in the contact forces at the initial stage of the impact. It was observed that the contact forces dropped after the peak of the first spike due to the separation of columns and the drop hammer. After the hammer came into contact with the columns, the columns moved slightly away from the hammer, causing the drop in the recorded contact force in the load cell. The hammer then moved downward and contacted the columns again increase the contact force and this process was repeated until the hammer and columns moved together where the load cell measured stable contact force. This phenomenon has also been observed by Eibl [8] when a striker impacted onto concrete structures.

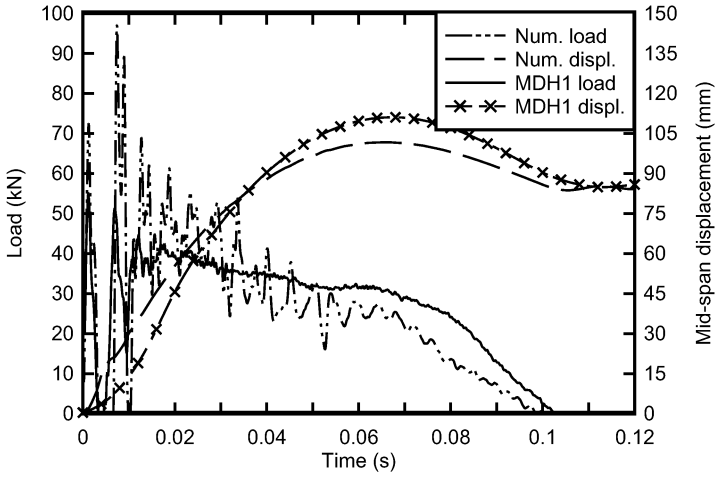

Figure 7: Comparison between numerical results and MDH1 experimental results.

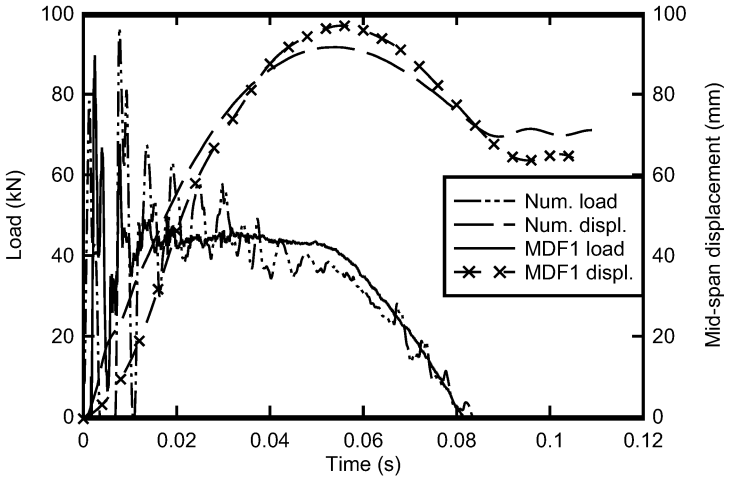

Figure 8: Comparison between numerical results and MDF1 experimental results.

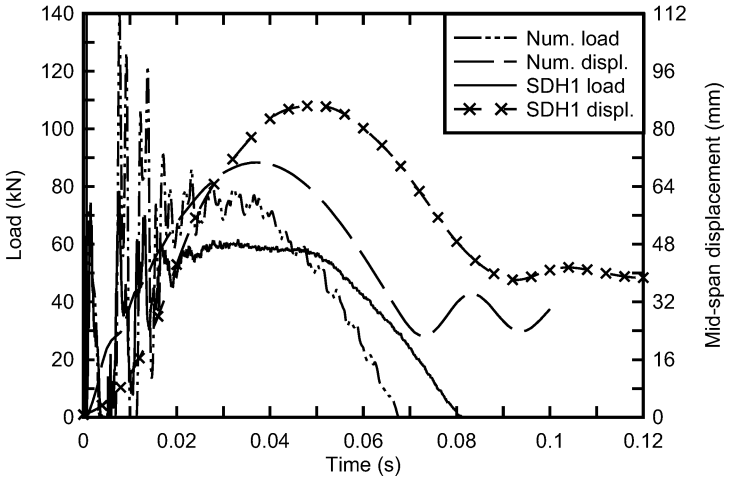

Figure 9: Comparison between numerical results and SDH1 experimental results

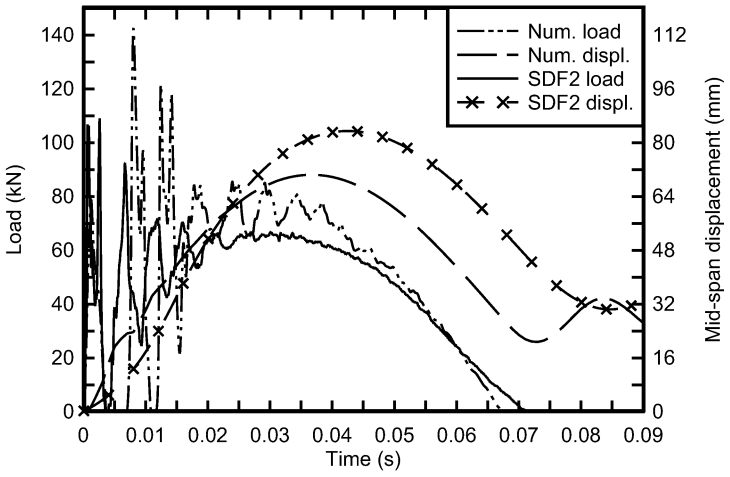

Figure 10: Comparison between numerical results and SDF1 experimental results

The buckling mode inferred by the numerical analyses corresponded well with that observed in the experimental results, as exemplified by the results for MDH1 illustrated in Figure 11. Both numerical and experimental results showed inward buckling of the flange impacted by the hammer and an outward buckling of side walls of MDH1.

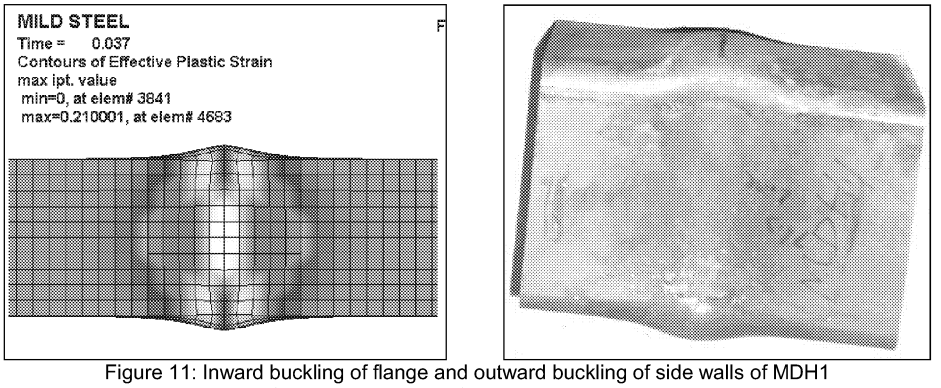

Figure 11: Inward buckling of flange and outward buckling of side walls of MDH1
(a) numerical result, (b) experimental result.

5. Conclusion

This paper presented the experimental results and numerical results from a simulation technique for hollow and PUR foam filled mild and stainless steel columns. Based on observations made in this research, some conclusions can be summarized as follows:

- Stainless steel columns demonstrated higher dynamic strength compared to the mild steel columns.
- The energy absorbing capacity of the foam filled columns is higher than that of the unfilled hollow sections, while the concrete filled columns have the highest energy absorbing capacity.
- For low velocity impact, the Cowper-Symonds coefficients for strain rate effects as employed in Material Type 24 of LS-Dyna can be ignored in the numerical simulations of impact events.
- Numerical models can satisfactory predict the impact load and displacement histories of hollow and foam filled columns under impact.

6. Acknowledgement

The authors wish to acknowledge the former honours student Grant Mete, Mitchell Hugo and Mr. Alan Grant from University of Wollongong for assisting with the experiments.

7. References

[1] Shim V.P.W, Tu Z.H, Lim C.T, Two-dimensional response of crushable polyurethane foam to low velocity impact. International Journal of Impact Engineering 24, 2000, p. 703-731.
[2] Tu Z.H, Shim V.P.W, Lim C.T, Plastic deformation modes in rigid polyurethane foam under static loading. International Journal of Solids and Structures 38, 2001, p.9267-9270.
[3] Chen W, Lu F, Winfree N. High-strain-rate compressive behaviours of a rigid polyurethane foam with various densities. Experimental Mechanics 30, 2001, p. 65-79.
[4] Lilley K and Mani A, Roof-crush strength improvement using rigid polyurethane foam. Journal of Materials Engineering and Performance 7, 1998, p. 511-514.
[5] Ismail A.E, Energy absorption of foam-filled steel extrusion under quasi-static oblique loading. International Journal of Engineering and Technology, Vol. 5, No. 1, 2008, p. 11-24.
[6] Sambamoorthy B, Halder T, Charaterization and component level correlation of energy absorbing (EA) polyurethane foams (PU) using LS-Dyna material models. 3rd European LS-DYNA Conference.
[7] Mullerschon H, Franz U, Munz T. Stander N, The identification of rate-dependent material properties in foams using LS-OPT. 7th International LS-DYNA Users Conferences, Salzburg, 14 - 15 May, 2009.
[8] Eibl J. Design of concrete structures to resist accidental impact. The Structural Engineering 1987, Vol 65A, p.27-32.